Mechanical and Thermo-Mechanical Studies of Double Networks Based on Thermoplastic Elastomers

NAVEEN K. SINGH, ALAN J. LESSER

University of Massachusetts at Amherst, Silvio O. Conte National Center for Polymer Research, Amherst, Massachusetts 01003-45303

Received 20 October 2009; revised 18 December 2009; accepted 19 December 2009
DOI: 10.1002/polb.21943
Published online in Wiley InterScience (www.interscience.wiley.com).

ABSTRACT: A new approach to prepare and characterize double network elastomeric systems was investigated. A styrene-ethylene-*co*-butylene-styrene (SEBS) triblock copolymer system containing physical crosslinks was used to achieve a double network by additional crosslinking using ultra-violet (UV) light. An ethylene–propylene–diene monomer (EPDM) terpolymer system containing chemical crosslinks was used to achieve a conventional double network using UV crosslinking. Properties from conventional monotonic tensile tests, dynamic mechanical analysis, and thermomechanical properties were investigated. These double network elastomers show a transition between competitive and collaborative behavior in their mechanical properties and lower coefficients of thermal expansion arising from a competition of the networks. © 2010 Wiley Periodicals, Inc. J Polym Sci Part B: Polym Phys 48: 778–789, 2010

KEYWORDS: crosslinking; elastomers; mechanical properties; networks; thermal properties

INTRODUCTION Traditional curing of a rubber or elastomer results in isotropic networks and properties.[1] From the kinetic theory, the elasticity of rubber has been attributed to the changes in the conformations and configurational entropy of a system of long-chain molecules. When the chains undergo deformation, the internal energy is considered to remain constant.[2] Hence, when loading and unloading the network, the heat exchange with the surroundings is due primarily to entropic contributions.

A general schematic of an elastomer's heat exchange with its surroundings, during deformation is shown in Figure 1. Heat is given out from the elastomer to the surroundings while loading, and is absorbed while unloading.

This heat exchange governs the mechanical and thermal properties of these networks. If a partially cured elastomer is first deformed and then subjected to additional crosslinking, a second crosslinked network can be formed within the initial network, as depicted in Figure 2. This results in materials with unusual and enhanced properties which have been termed "double network elastomers."[1,3–6] These properties arise from a competition between these two networks during small deformations, where heat released by one network is being absorbed by the other network. Thus, a lower modulus is expected in this low strain, competitive regime relative to a single network system. At higher elongations these networks work in parallel to each other to provide a collaborative behavior, and consequently a higher modulus than in a single network system is expected.

Because of entropic dependence of these elastomers, the stretched rubber is expected to have a lower coefficient of thermal expansion in the stretched direction. Therefore, these systems can be very useful in applications where positive thermal expansion must be reduced, without using a composite material exhibiting a negative coefficient of thermal expansion.[7]

The concept of a double network was introduced more than 50 years ago by Tobolsky and coworkers.[4] Their studies explained the physical ageing of rubbers, which involved free-radical scission and crosslinking under deformation, and the independent network hypothesis they proposed has been rigorously proved.[8–14] This hypothesis suggested that the constitutive relation for postcured networks can be calculated as the sum of the stress contributions from the independent networks, each described by the classical stress–strain expression. Each independent network has its own state of equilibrium.

Flory[8] proposed a very general theoretical treatment of similar systems and his expression for the elastic free energy of the double network system, assuming Gaussian chains, is given in eq 1.

$$\frac{\Delta F_{el}}{RT} = \left(\frac{\upsilon_1}{2}\right)(\lambda_x^2 + \lambda_y^2 + \lambda_z^2 - 3) + \left(\frac{\upsilon_2}{2}\right)(\lambda_{x:2}^2 + \lambda_{y:2}^2 + \lambda_{z:2}^2 - 3) - \left(\frac{1}{2}\right)(\upsilon_1 + \upsilon_2)\ln\left(\frac{V}{V_0}\right) \quad (1)$$

Correspondence to: A. J. Lesser (E-mail: ajl@polysci.umass.edu)

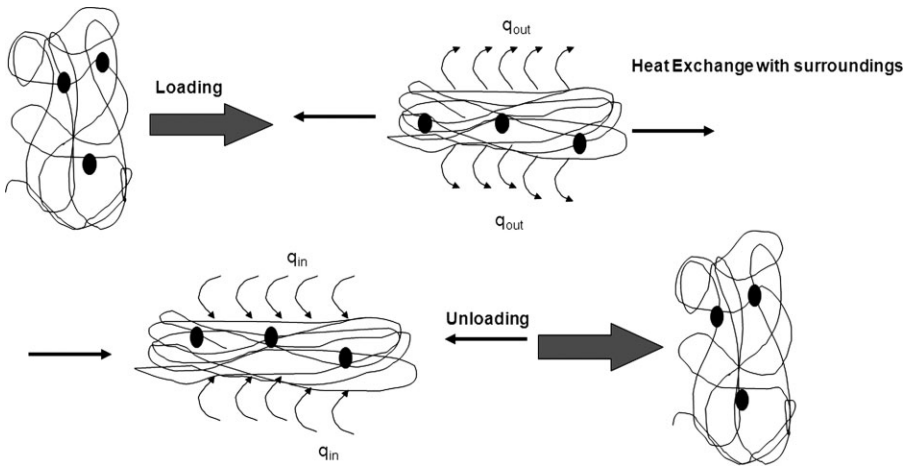

FIGURE 1 Heat exchange with the surrounding for traditional isotropic network.

where

λ_x, λ_y, and λ_z = extension ratios relative to the initial isotropic state;

$\lambda_{x:2}$, $\lambda_{y:2}$, and $\lambda_{z:2}$ = extension ratios relative to the state in which the second set of crosslinks is introduced;

V = the actual volume;

V_o = the reference volume;

υ_1 = number of elastically effective strands between crosslinks in the isotropic unstretched state;

υ_2 = number of additional elastically effective strands between crosslink in the cured sample at a stretched state;

In this scheme, there are two opposing forces acting on this system. One is due to the network introduced in the isotropic state, and the other is due to the network introduced in the strained stat; thus there is a stress transfer between these networks.

Flory also proposed a theory to explain double network systems using protein fibers.[15] Baxandall and Edwards[16] carried out theoretical treatment to explain deformation-dependent properties of polymer networks constructed by addition of crosslinks under strain. Toughness improvements were theoretically proven by Okumura,[17] and Meissner and Matjka[18] provided a Langevin-elasticity-theory-based description of the tensile properties of double network rubbers. Molecular dynamics simulation studies were also carried out on these double network elastomers to understand and explain permanent set.[19–23]

Until recently, the concept of double network elastomers was confined to studies of the physical ageing of elastomers. In the last 2 decades, many studies probed the physical properties of double networks, with the intent of applying them to practical applications. Properties studied included stress relaxation behavior,[24] orientation and crystallization effects,[1,25] electrical conductivity,[26] tensile properties,[27] fatigue,[28] birefringence,[29] creep-recovery,[30,31] swelling,[32,33] failure properties,[34] dynamic properties, and filler effects.[35] However, little attention has been given to the thermal and thermomechanical behavior, despite their significance in applications such as *o*-rings, actuators, encapsulants, and dampers. Moreover, there has been almost very little work in the field of thermoplastic elastomers.

Thermoplastic elastomers (TPEs) have recently been studied as a possible replacement for traditionally cured elastomers. They follow the thermodynamic behavior similar to traditional elastomers, and their deformational behavior has been studied in the group.[36,37] TPEs are generally block copolymers, having hard and soft segments. In contrast to the traditionally cured elastomers, which once cured cannot be reshaped, TPEs provide ease of processibility to give rubbery materials which can be reshaped again, like other thermoplastics. However, TPEs lack thermal stability and their rigidity is limited by the stiffness of hard block.[38] Nonetheless, the thermoelastic properties of TPEs make them an interesting competitor to traditional elastomers.

In this work, initial results are presented from an ongoing investigation[39,40] aimed to elucidate the mechanisms behind the mechanical and thermomechanical behavior of competitive double network thermoplastic elastomers. Herein, a double-networked styrene-ethylene-*co*-butylene-styrene (SEBS) triblock copolymer is prepared by using physical crosslinks from the hard styrenic phase as the first network and curing it in a deformed state to achieve a second chemically

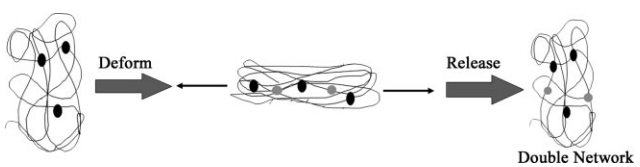

FIGURE 2 Formation of double network.

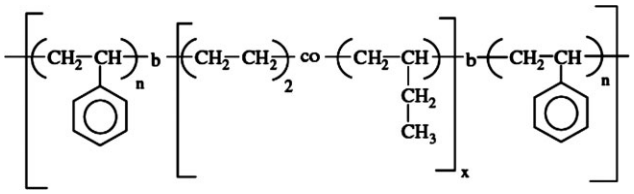

FIGURE 3 Chemical structure of SEBS.

crosslinked network. To compare the double networks formed from physical crosslinks and from chemical crosslinks, a double-networked ethylene-*co*-propylene-diene-monomer (EPDM) terpolymer was also prepared, by utilizing only the chemical crosslinks from the unsaturation. The properties of these materials are compared at similar total crosslink times, but at different extension ratios before imposing the second network.

EXPERIMENTAL

Materials

SEBS triblock copolymer was obtained from Kraton®. The general structure is shown in Figure 3, containing 20% polystyrene in the endblocks and 20% polystyrene in mid blocks.

EPDM terpolymer was obtained from Exxon Mobil® and its general structure is shown in Figure 4. The diene monomer present in the EPDM was ethylene norbornene (ENB), at a concentration of 2.8% by weight.

Both SEBS and EPDM were mixed with 5% benzophenone (Alfa Aesar), a UV crosslinking initiator, and melt blended using a Brabender batch mixer at 250 and 150 °C, respectively. Films with a thickness of ~0.5–1 mm were obtained by melt pressing at 260 °C for SEBS and at 150 °C for EPDM. ASTM D638 type IV tensile samples were punched out of the films.

Double-Network Formation

Double networks of SEBS were prepared by UV crosslinking using an Atlas Suntest CPS+. The first network results from the physical networks of the hard polystyrene block and is present immediately after processing. The second network was introduced by first uni-axially extending the sample to prescribed extension ratios (λ^c = 1.5, 2, 3, and 4), and subsequently curing it using UV radiation. This one-step UV curing was carried out after optimizing the curing conditions to a dosage power of 500 W/m^2 at 25 °C for 8 h to give a total dosage of 14,400 kJ/m^2. The optimization was carried out by varying time and dosage to attain saturation in the modulus values of single network systems by varying time and dosage. After curing, samples were allowed to relax back to their equilibrium state.

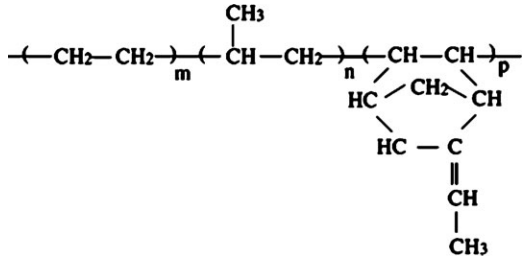

FIGURE 4 Chemical structure of ENB-based EPDM.

TABLE 1 Cure Schemes to Prepare SEBS and EPDM Double Network Elastomers

	SEBS	EPDM
Primary network	Already present (Physical crosslinks)	Formed by partial UV curing (Chemical crosslinks)
Secondary network	Formed by UV curing while stretched at λ^c = 1–4 (Chemical crosslinks)	Formed by UV curing while stretched at λ^c = 1–4 (Chemical crosslinks)

EPDM double networks were also prepared by UV crosslinking. The first network in the double network resulted from UV curing for 20 min at a dosage of 700 W/m^2 at 25 °C to give a total dosage of 840 kJ/m^2. The second network was introduced by uni-axially extending the precured sample to prescribed extension ratios (λ^c = 1.5, 2, 3, and 4), and subsequently curing it using UV radiation for 40 min at a dosage of 700 W/m^2 at 25 °C to give a total dosage of 1680 kJ/m^2. The curing characteristics of EPDM were not optimized. After curing, samples were allowed to relax back to their equilibrium state.

The difference between the SEBS and the EPDM double network samples is that the first network in SEBS is a physical crosslink, whereas chemical crosslinks form the first network of EPDM. The second network in both the cases is formed by chemical crosslinking. The relevant differences between SEBS and EPDM double network elastomers are depicted in Table 1.

These double network samples were compared with samples cured at λ^c = 1, which did not undergo any extension between the first and second cure.

Mechanism of Crosslinking

The mechanism of free-radical crosslinking and oxidation in SEBS has been investigated[41–43] and it was found that upon exposure to UV, both styrenic and olefinic phases undergo degradation, resulting in discoloration and loss of properties. This mechanism is shown in Figure 5. Rapid hydroperoxide growth was observed in the olefinic phase, with subsequent oxidation and end-chain scission at the boundary of the styrene-olefin phases. The growth and build-up of the hydroperoxide is very low, indicating that the reaction is confined to the surface layer of the polymeric material. Crosslinking reactions were also minimal. To stabilize the material and increase the crosslinking, a crosslinking initiator such as

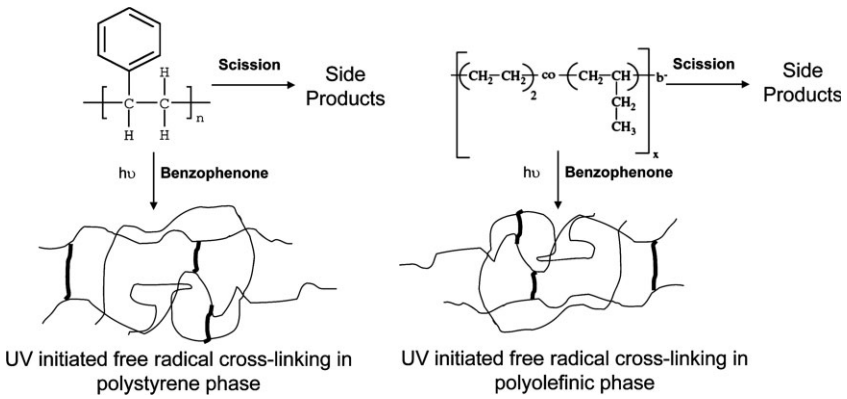

FIGURE 5 Free radical crosslinking mechanism in styrenic and olefinic phase.

benzophenone was used.[44] Using benzophenone can result in an increase in crosslinking in both styrenic as well as olefinic phases, and reduce the scission reactions.

The photo crosslinking of EPDM has also been studied,[35,45–48] and the mechanism is shown in Figure 6. A photoinitiator such as benzophenone is used to crosslink the ethylene norbornene unsaturation.

Infra-Red Spectroscopy

Fourier transform infrared (FTIR) spectroscopy was utilized to qualitatively determine the extent of crosslinking. Infrared spectra were obtained on a Perkin–Elmer Spectrum One FTIR spectrometer.

Mechanical Properties

Monotonic uniaxial tensile properties were determined using an Instron 4411 tensile test machine, at a constant crosshead speed of 20 mm/min at 23 °C. ASTM D1708 test geometry was used for all the samples used for mechanical testing as shown in Figure 7.[49] Samples were tested in the direction parallel to the direction of stretch during cure.

The engineering stress versus extension ratio curves were plotted for these double networks, where extension ratios (λ^t) were calculated based on the final equilibrium length of these double networks. These stress versus extension ratio curves were used to calculate the effective crosslink density, which contains a contribution attributed to chain entanglements and loose chain ends acting as crosslinks in rubber. The effective crosslink density was calculated according to the Mooney–Rivlin equation, shown in eq 2.

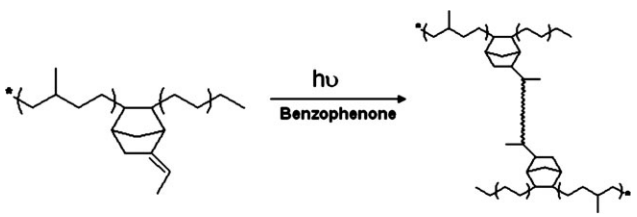

FIGURE 6 Free radical crosslinking mechanism via norbornene unsaturation of EPDM.

$$\upsilon = \frac{\sigma}{2RT\left(\lambda^t - \frac{1}{\lambda^{t2}}\right)} \quad (2)$$

where

υ = the effective crosslink density;
σ = the engineering stress;
R = the universal gas constant;
T = the absolute temperature;
λ^t = the extension ratio of the sample.

Dynamic Mechanical Analysis

Dynamic mechanical properties were determined using a Dynamic Mechanical Analyzer (TA Instruments-DMA 2980) at a constant frequency of 1 Hz and 0.1% strain. Thin film samples were oscillated in the direction parallel to the stretch direction during cure, over a temperature range of −80 to 250 °C, ramped at 5 °C/min.

Thermo-Mechanical Properties

Thermo-mechanical properties, including the thermal stability under load and coefficient of thermal expansion, were

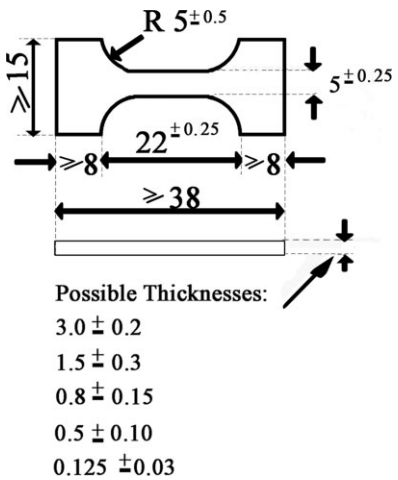

FIGURE 7 Specimen geometry for the ASTM D 1708 standard.

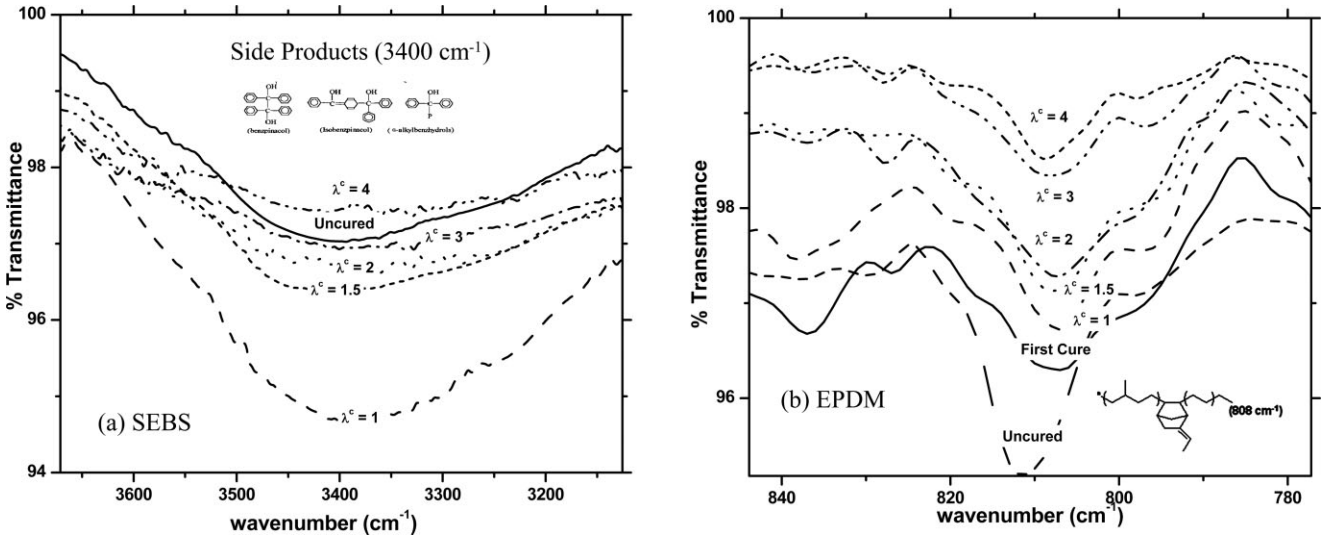

FIGURE 8 Infrared spectrograph (a) SEBS double network and (b) EPDM double network, each compared with samples with $\lambda^c = 1$.

studied using the film/fiber probe in TA instrument Thermo-Mechanical Analyzer (TMA) 2940CE, at constant load of 0.05 N and heating rate of 3 °C/min.

RESULTS AND DISCUSSION

Extent of Crosslinking

The extent of crosslinking in both SEBS and EPDM was determined qualitatively using infrared spectroscopy. The peak chosen to compare the different samples of SEBS was at 3400 cm^{-1}, which corresponds to the hydroxyl-group based side products which are formed in competition with the crosslinking reaction. Hence, higher peak intensity corresponds to lower extent of crosslinking. The peak chosen to compare the different samples of EPDM was at 808 cm^{-1}, which corresponds to the norbornene unsaturation. Hence, higher peak intensity corresponds to higher extent of crosslinking. In both systems, the chosen peak intensity decreases with an increase in λ^c, as shown in Figure 8.

The increase in extent of curing can be attributed to decrease in thickness and increase in surface area available for UV crosslinking when the samples are stretched to higher λ^c. As UV crosslinking is governed by the penetration depth, a lower thickness will lead to a higher extent of crosslinking. Polymer chain orientation causes crowding of chains and there is a higher probability of two chains combining together to form a crosslink than leading to other side scission reactions.

Tensile Response

SEBS samples were stretched to various λ^c and then cured. Whereas EPDM samples were partially cured and then extended to λ^c before curing them further. The percent permanent set and the residual extension ratio of the various double-networked rubbers, along with their mechanical properties, are given in Tables 2 and 3. The residual strain and permanent set were calculated based on eqs 3 and 4, respectively.[4]

$$\varepsilon_R = \frac{1_s}{1_u} \tag{3}$$

$$\varepsilon_P = \left(\frac{l_s - l_u}{l_x - l_u}\right) \tag{4}$$

where

ε_R = Residual Strain
ε_P = Permanent Set
l_s = Set length
l_u = Unstretched Length
l_x = Stretched Length

TABLE 2 Summary of Mechanical Properties of SEBS Samples Cured at Different λ^c

λ^c	Permanent Set (ε_P)	Residual Strain (ε_R)	Initial Modulus (MPa)	Final Modulus (MPa)	Elongation at Break (%)	Toughness (MPa)
1	–	1.00	10.63	2.6	130	3.23
1.5	0.72	1.36	9.35	3.7	150	5.46
2	0.57	1.57	7.55	4.6	133	4.25
3	0.56	2.12	7.03	7.1	103	3.33
4	0.49	2.48	6.88	8.8	118	4.58

TABLE 3 Summary of Mechanical Properties of EPDM Samples Cured at Different λ^c

λ^c	Permanent Set (ε_P)	Residual Strain (ε_R)	Initial Modulus (MPa)	Final Modulus (MPa)	Elongation at Break (%)	Toughness (MPa)
1	–	1.00	3.65	1.68	318	3.58
1.5	0.74	1.37	3.04	1.83	183	1.87
2	0.67	1.67	2.81	2.02	136	1.41
3	0.57	2.14	3.56	2.28	100	1.09
4	0.52	2.56	3.35	2.36	121	1.96

The aforementioned parameters are shown in Figure 9.

From Tables 2 and 3, it is evident that there is a significant improvement in overall mechanical properties of double networks formed in a stretched state as opposed to an unstretched state ($\lambda^c = 1$). Figure 10 shows uniaxial stress versus λ^t curves for the SEBS double network systems. Samples tested were single network (uncured) and double networks prepared at $\lambda^c = 1$, 1.5, 2, 3, and 4. It is evident from Figure 10(a) that, even having the same crosslink time in all the cured samples, the double network samples exhibit higher ultimate modulus compared with both the uncured and the $\lambda^c = 1$ double network. This agrees with independent network hypothesis. Analyzing the data carefully, it is evident from Figure 10(b) that there is a transition in modulus detectable in the double network elastomer which is absent in both the uncured sample and the sample cured at $\lambda^c = 1$. This is due to the fact that, below the transition point, the two networks are in competition with each other, while above it, they become collaborative and act in parallel, leading to an increase in modulus. The position of the transition point is dependent on λ^c.

Compared with the uncured polymer, the samples cured at $\lambda^c = 1.5$ and 2 show a lower modulus at lower λ^t and a higher modulus at higher λ^t, but do not exhibit strain hardening at higher λ^t. Samples cured at $\lambda^c = 3$ and 4 show an initial drop, as compared to the one cured at $\lambda^c = 1$, followed by an increase in the modulus, along with strain hardening. The decrease in initial modulus, while carrying out monotonic uniaxial tensile test in all the samples is a result of the competitive behavior of the two networks and due to heat exchange between these networks. The samples cured at higher λ^c shows strain hardening behavior at a lower λ^t value as compared to the one cured at $\lambda^c = 1$, hence indicating the permanent anisotropy embedded in the double network elastomer. This results in increase in the modulus of the double networks even at moderate λ^t.

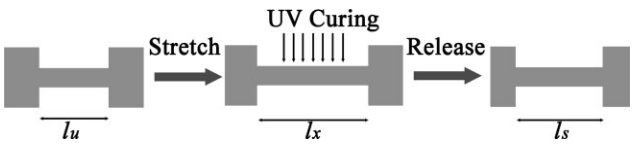

FIGURE 9 Diagram representing various parameters used to calculate permanent set and residual strain.

Similar behavior was observed in the case of EPDM as shown in Figure 11(a). There is an increase in modulus with increase in λ^c, at values of λ^t beyond the transition points as shown in Figure 11(b). As the curing conditions of the EPDM double network samples have not been optimized, the transition points are not easily separated and are very low due to incomplete curing.

This nonlinear behavior is also evident from the Mooney–Rivlin curve shown in Figure 12, where the reduced stress $\left[\frac{\sigma}{(\lambda^t - \frac{1}{\lambda^{t2}})}\right]$ is plotted against the inverse of λ^t. It is observed that the SEBS double network elastomers are highly nonlinear systems, whereas EPDM samples are more linear. SEBS samples show nonlinear behavior at smaller λ^t as compared to the uncured samples and the samples cured at $\lambda^c = 1$, and this nonlinear behavior increases with an increase in λ^c. EPDM double network samples show slight nonlinearity with increase in λ^c.

On the basis of the Mooney–Rivlin equation, the concentrations of physically effective crosslinks were calculated and are shown in Figure 13. The best fit was calculated based on the linear region of the Mooney–Rivlin plot. Even with the same curing dosages, the crosslink density increases with increase in λ^c. This is in agreement with the FTIR results and can be attributed to the increase in surface area and decrease in thickness with increase in λ^c. This also concurs with an increase in the polymer chain orientation, leading to higher probability of crosslinking reactions as compared with chain scission reactions.

Dynamic Mechanical Analysis

The introduction of double networks changes the modulus of the material. The storage modulus values for SEBS and EPDM samples are plotted against temperature for samples cured at different λ^c, as shown in Figures 14 and 15. The graphs can be divided into three distinct regions: the glassy region, the transition (leathery) region, and the rubbery region. The plateau modulus in the rubbery region is lower for double-networked samples cured at higher λ^c. Hence, the storage modulus curves follow the thermodynamic behavior and are governed by the entropy of the system. The drop in storage modulus plateau with an increase in λ^c may be associated with the competitive nature of the two networks formed in the sample, which was strained at a very small strain and at low frequency. This causes a decrease in overall

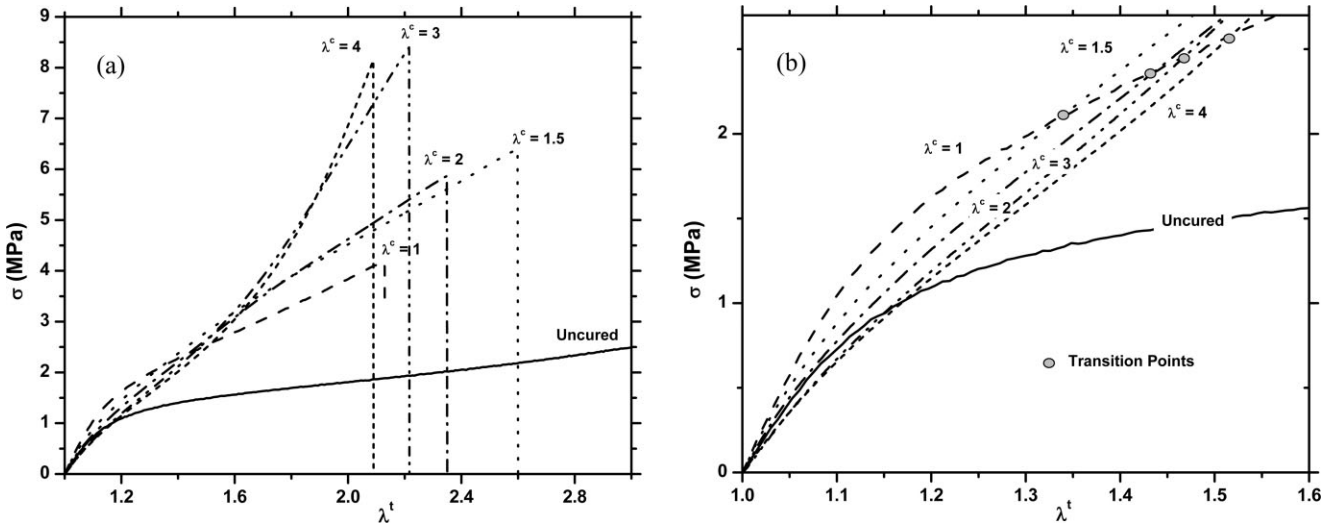

FIGURE 10 Tensile results of SEBS samples cured at different λ^c (a) Full stress-extension results, (b) Closeup of low extension regime.

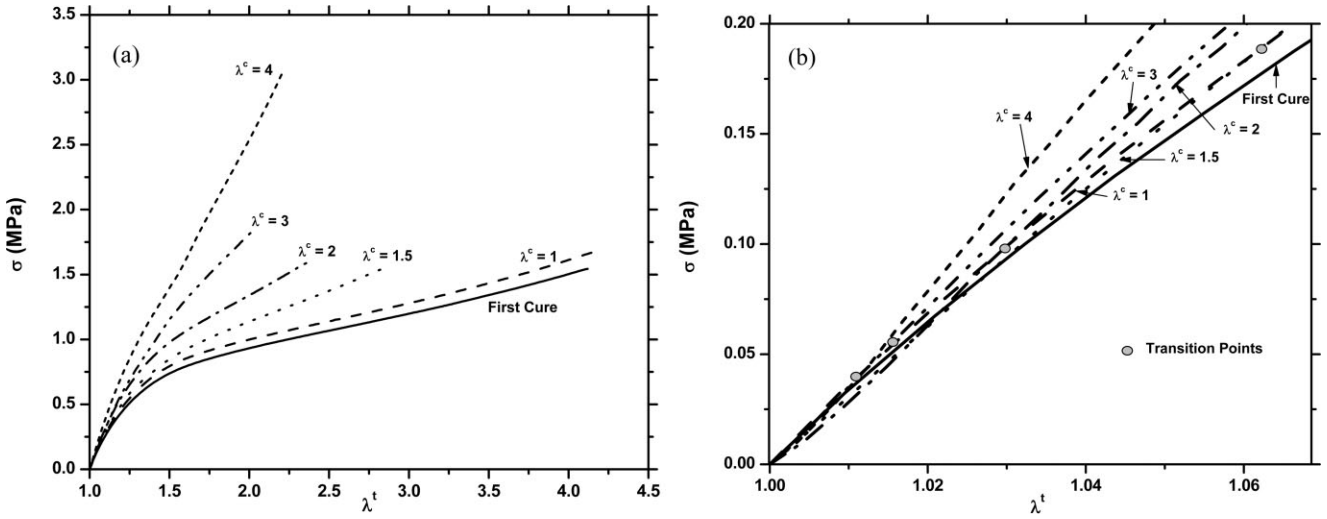

FIGURE 11 Tensile results of EPDM samples cured at different λ^c (a) Full stress-extension results, (b) Closeup of low extension regime.

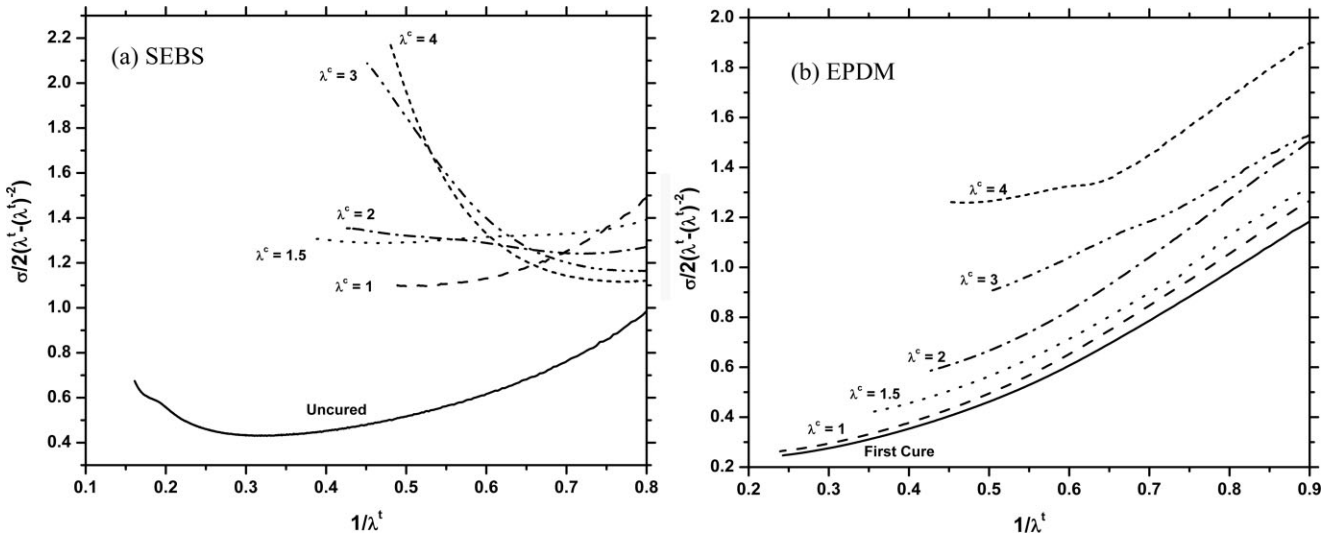

FIGURE 12 Mooney–Rivlin plot (a) SEBS, (b) EPDM; corresponding to Figures 10 and 11.

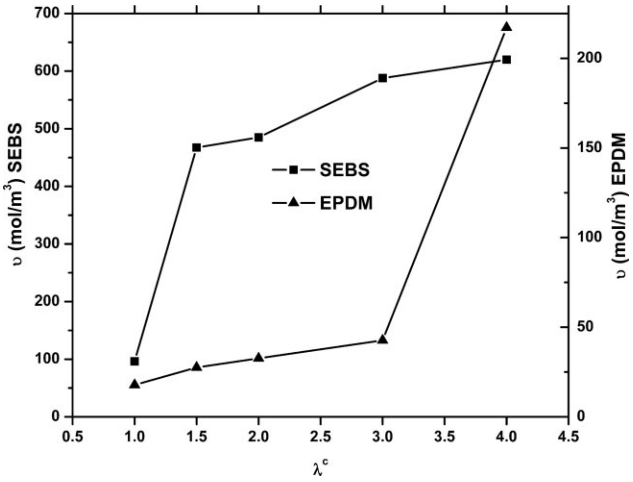

FIGURE 13 Physical effective crosslink densities of double network SEBS and EPDM calculated from the Mooney–Rivlin plot shown in Figure 12.

modulus of the double network system in the rubbery region of the elastomer.

The loss modulus values versus temperature for SEBS and EPDM are shown in Figure 16. In the rubbery regions of both the SEBS and EPDM double network, the loss modulus of the networks decreases with increase in λ^c. Even in the glassy regime there is slight decrease in the loss modulus, which suggests that there is an increase in crosslinking with increase in λ^c. This also suggests that there is less viscous behavior of the samples with higher degree of crosslinking.

Crosslinking increases the glass transition temperature (T_g) of a polymer by introducing restrictions in the molecular motions of the chains. The plot of tan δ as a function of temperature for SEBS and EPDM is shown in Figure 17. The peak of the curve is taken as the T_g. The T_g values of both

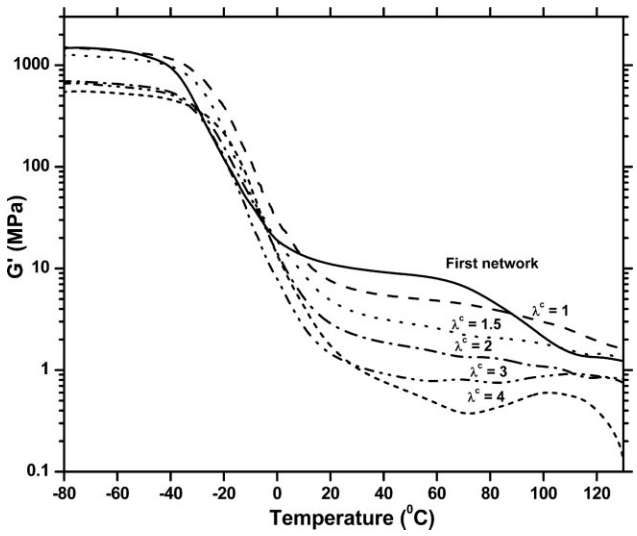

FIGURE 14 Storage modulus of the double network SEBS samples.

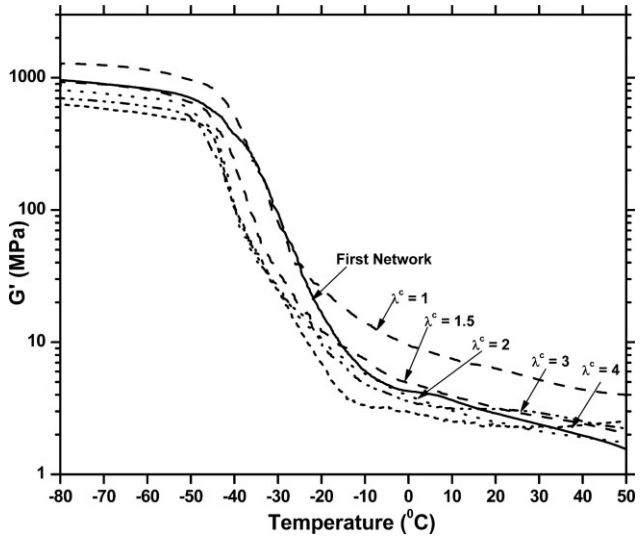

FIGURE 15 Storage modulus of the double network EPDM samples.

the polyolefin and the polystyrene phases show an increase with increase in crosslink density for SEBS. EPDM also exhibits an increase in T_g. This increase in T_g can be explained on the basis of increase in crosslink density with increase in λ^c and negligible effect of orientation of chains as studied by Munch et al.[50] The peak area is a measure of mechanical damping ability[27] and can be related to the service performance of the products. A slight increase in damping is observed in both SEBS and EPDM as shown in Figure 18, with an increase in λ^c. This may be attributed to the competitive nature of the networks in the low strain regime, and may lead to better fatigue life as shown by Santangelo and Roland.[28]

The tan δ and loss modulus curves appear to correlate with true crosslink densities, showing an increase in crosslinking with increase in λ^c. However, the storage modulus follows the competitive behavior of the double network and hence decreases in the low λ^t regime with an increase in λ^c.

Thermo-Mechanical Analysis

The dimensional change measured at constant load as a function of temperature is shown in Figure 19. The coefficient of thermal expansion (CTE) was calculated using the following equation:

$$\alpha = \frac{\Delta L \times K}{\Delta T \times L} \tag{5}$$

where

α = coefficient of expansion (μm/mm °C);
L = sample length (mm);
ΔL = change in sample length (μm);
ΔT = change in temperature (°C);
K = cell constant.

It is evident that the curing at $\lambda^c = 1$ leads to a decrease in the coefficient of thermal expansion (CTE) of both SEBS and

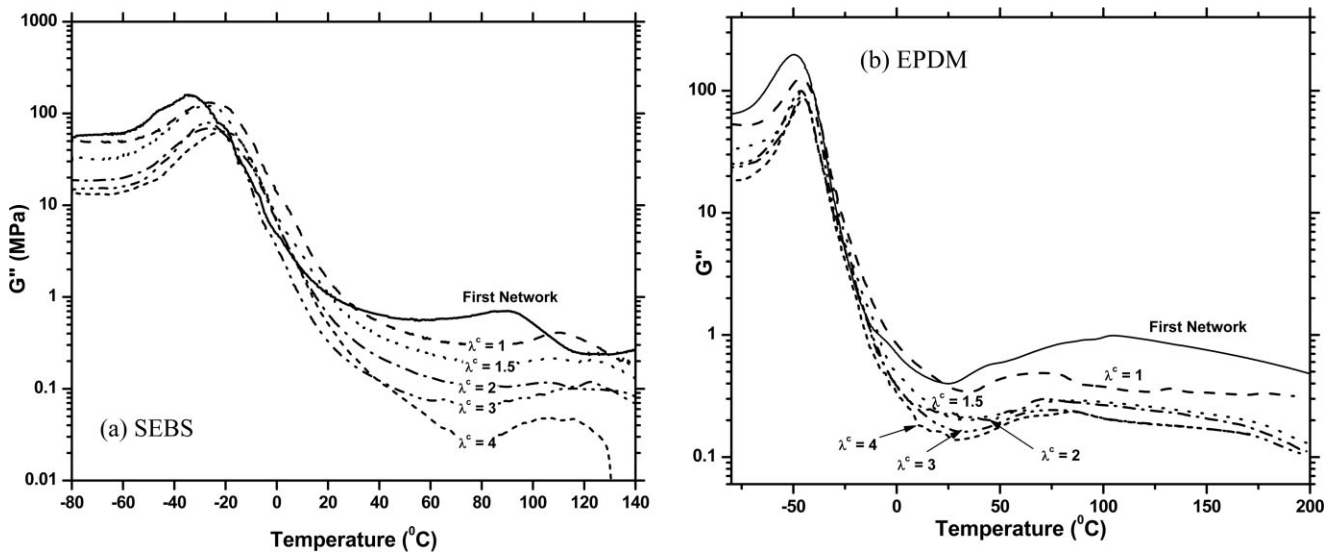

FIGURE 16 Loss modulus of the double network (a) SEBS and (b) EPDM samples as compared to samples with $\lambda^c = 1$.

EPDM samples and an improved thermal stability under load as compared to the uncured sample. Hence, it may be suitable for high temperature applications.

It is also evident that the samples cured at various λ^c shows interesting behavior along with increase in temperature. All the SEBS samples with $\lambda^c = 1$–4 show a transition at ~55–60 °C, at which only the physically crosslinked uncured samples failed. The CTE values of all the samples, before and after the transition point, are given in Table 4. The CTE values before the transition point are positive for the sample cured at $\lambda^c = 1$. The samples cured at higher λ^c show a decrease in CTE and in the case of $\lambda^c = 4$, it almost reaches zero. This can be attributed to that fact that the second network is leading to increase in anisotropy in the direction of stretch due to an increase in residual strain. They also show a transition at ~55–60 °C, beyond which a negative CTE is obtained. This may be due to the expansion of the double network elastomers before the transition point, with both the networks contributing in the expansion. However, beyond the transition point, where one of the networks fails, the second network tries to attain equilibrium, and following entropic behavior, contracts, which is seen as a negative CTE value. The negative CTE values also increase with increasing λ^c.

Similar behavior is observed in the case of EPDM. The double network elastomers show a negative CTE and there is a transition point at ~45 °C, beyond which the slope decreases further. The CTE values of all samples, before and after the transition point, are given in Table 5. The samples do not show a contraction after failure of the first network because both networks are formed from chemical crosslinks.

The first explanation of this kind of behavior of elastomers was given by Govi to explain the Joule effect, where

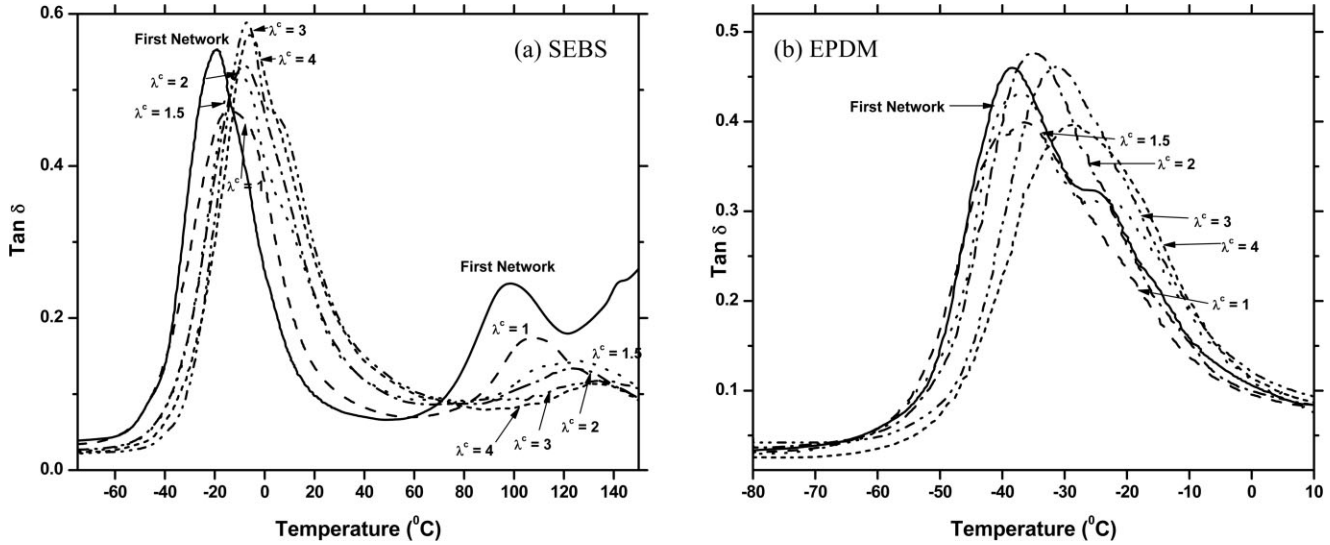

FIGURE 17 Tan δ of the double network (a) SEBS and (b) EPDM samples as compared to samples with $\lambda^c = 1$.

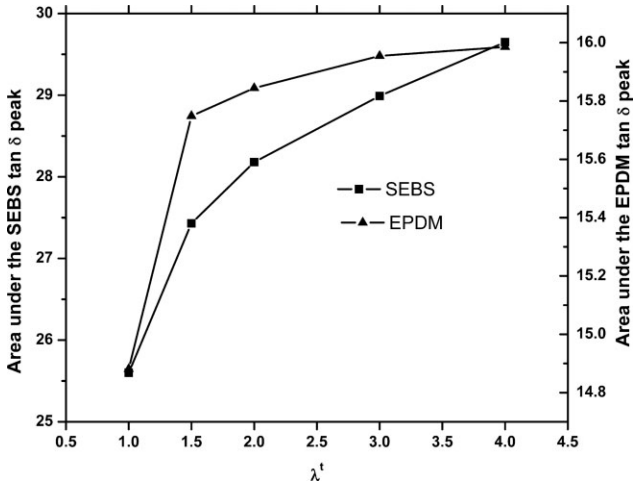

FIGURE 18 Increase in area under the olefenic tan δ peak of SEBS and EPDM with increase in λ^c.

elastomers show a contraction when they are under strain. He assumed rubber as a "sort of solid foam composed of innumerable vesicles full of gas." On stretching the rubber, according to him, the vesicles stretch in the direction of extension and contract in the perpendicular direction. On application of heat, the gas in the vesicles will result in expansion and each vesicle would want to return to its original minimized free energy state of a sphere. This would lead to linear contraction.[51] The analogy to the gaseous behavior of rubbers suggests the entropic dependence of these elastomers. These double networks hence have stretched chains, frozen in the system, by introducing the second network in stretched state, which lead to contraction upon heating, even with higher crosslinking densities.

TABLE 4 Summary of Coefficient of Thermal Expansion of SEBS

λ^c	α Before Transition (μm/mm °C)	α After Transition (μm/mm °C)
1	0.60	1.81
1.5	0.33	−1.04
2	0.58	−1.55
3	0.24	−2.45
4	0.020	−2.47

CONCLUSIONS

SEBS- and EPDM-based double networks have been formed and investigated. In both systems, a competitive regime and a collaborative regime have been identified, and the transition point is related to elongation of the sample during the formation of the second network. The storage modulus decreases in the competitive regime, even though crosslink density and T_g increase and loss modulus decreases. This indicates the competitive regime is purely entropic and independent of the network changes, as observed between the physical networks for SEBS and chemical networks for EPDM. Constitutive equations governing this behavior are still to be investigated. These double network systems also form stiffer materials with higher crosslinking densities, yet show a lower or even a negative coefficient of thermal expansion, without addition of any filler. This is due to the entropic restrictions in this class of material. These materials

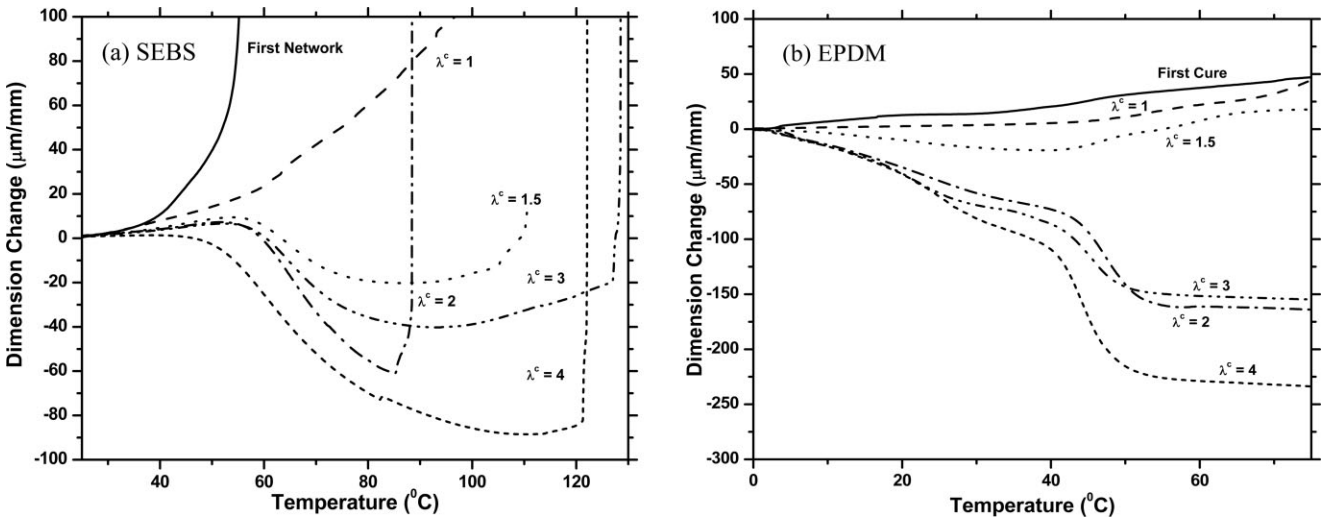

FIGURE 19 TMA results of (a) SEBS, (b) EPDM double network samples cured at different λ^c at constant load of 0.05 N and temperature ramp rate of 3 °C/min.

TABLE 5 Summary of Coefficient of Thermal Expansion of EPDM

λ^c	α Before Transition (μm/mm °C)	α After Transition (μm/mm °C)
1	0.112	1.17
1.5	−0.61	1.16
2	−2.442	−5.39
3	−2.832	−6.83
4	−2.914	−9.03

can be very useful in many industrial applications such as lamination, where a balance of stiffness and expansion coefficient is required. They also have the potential to show improvement in other properties, such as fatigue and toughness, because of a high dependence on the entropic behavior of chains. These properties, along with the thermodynamics of these systems are still to be investigated.

The authors gratefully acknowledge Kathryn Wright, Kraton Polymers LLC for and Sudhin Datta, Exxon Mobil for providing the materials used in this study.

REFERENCES AND NOTES

1 Roland, C. M.; Warzel, M. L. Rubber Chem Technol 1990, 63, 285–297.

2 Treloar, L. R. G. The Physics of Rubber Elasticity; Oxford University Press: London, England, 1975.

3 Santangelo, P. G.; Roland, C. M. Rubber Chem Technol 1994, 67, 359–365.

4 Andrews, R. D.; Tobolsky, A. V.; Hanson, E. E. J Appl Phys 1946, 17, 352–361.

5 Baldwin, F. P.; Woodbridge, N. J. U.S. Pat. 2,488,112 (1945).

6 Erman, B. Biol Synth Polym Networks 1988, 497, 497–508.

7 Miller, W.; Smith, C. W.; Mackenzie, D. S.; Evans, K. E. J Mater Sci 2009, 44, 5441–5451.

8 Flory, P. J. Trans Faraday Soc 1960, 56, 722–743.

9 Kramer, O.; Ty, V.; Carpente, R. L.; Ferry, J. D. Bull Am Phys Soc 1973, 18, 318–318.

10 Kramer, O.; Carpenter, R. L.; Ty, V.; Ferry, J. D. Macromolecules 1974, 7, 79–84.

11 Carpenter, R. L.; Kramer, O.; Ferry, J. D. Bull Am Phys Soc 1977, 22, 429–429.

12 Carpenter, R. L.; Kramer, O.; Ferry, J. D. Macromolecules 1977, 10, 117–119.

13 Carpenter, R. L.; Kramer, O.; Ferry, J. D. J Appl Polym Sci 1978, 22, 335–342.

14 Berry, J. P.; Scanlan, J.; Watson, W. F. Trans Faraday Soc 1956, 52, 1137–1151.

15 Flory, P. J. J Am Chem Soc 1956, 78, 5222–5234.

16 Baxandall, L. G.; Edwards, S. F. Macromolecules 1988, 21, 1763–1772.

17 Okumura, K. Eur Lett 2004, 67, 470–476.

18 Meissner, B.; Matjka, L. Polymer 2003, 44, 4611–4617.

19 Budzien, J.; Rottach, D. R.; Curro, J. G.; Lo, C. S.; Thompson, A. P. Macromolecules 2008, 41, 9896–9903.

20 Rottach, D. R.; Curro, J. G.; Budzien, J.; Grest, G. S.; Svaneborg, C.; Everaers, R. Macromolecules 2006, 39, 5521–5530.

21 Rottach, D. R.; Curro, J. G.; Budzien, J.; Grest, G. S.; Svaneborg, C.; Everaers, R. Macromolecules 2007, 40, 131–139.

22 Rottach, D. R.; Curro, J. G.; Grest, G. S.; Thompson, A. P. Macromolecules 2004, 37, 5468–5473.

23 Svaneborg, C.; Everaers, R.; Grest, G. S.; Curro, J. G. Macromolecules 2008, 41, 4920–4928.

24 Gillen, K. T. Macromolecules 1988, 21, 442–446.

25 Roland, C. M.; Santangelo, P. G. World Pat. 95/26,367 (1995).

26 Roland, C. M.; Peng, K. L. Rubber Chem Technol 1991, 64, 790–800.

27 Aprem, A. S.; Joseph, K.; Thomas, S. J Appl Polym Sci 2004, 91, 1068–1076.

28 Santangelo, P. G.; Roland, C. M. Rubber Chem Technol 2003, 76, 892–898.

29 Mott, P. H.; Roland, C. M. Macromolecules 2000, 33, 4132–4137.

30 Kaang, S.; Gong, D.; Nah, C. J Appl Polym Sci 1997, 65, 917–924.

31 Kaang, S.; Nah, C. Polymer 1998, 39, 2209–2214.

32 Kaang, S.; Gong, D.; Nah, C.; Kim, S.; Kim, J. M. Polym Korea 1997, 21, 282–288.

33 Marykut-Ry, C. V.; Mathew, G.; Thomas, S. Rubber Chem Technol 2007, 80, 809–819.

34 Santangelo, P. G.; Roland, C. M. Rubber Chem Technol 1995, 68, 124–131.

35 Wang, J.; Hamed, G. R.; Umetsu, K.; Roland, C. M. Rubber Chem Technol 2005, 78, 76–83.

36 Indukuri, K. K.; Lesser, A. J. Polymer 2005, 46, 7218–7229.

37 Wright, K. J.; Indukuri, K.; Lesser, A. J. Polym Eng Sci 2003, 43, 531–542.

38 Holden, G.; Legge, N. R.; Quirk, R.; Schroeder, H. E. Thermoplastic Elastomers; Hanser/Gardner Publications, Inc.: Cincinnati, 1996.

39 Singh, N. K.; Lesser, A. J. Soc Plast Eng Annu Tech Conf 2009, 67, 868–873.

40 Lesser, A. J.; Singh, N. K.; Mamodia, M. (to University of Massachusetts, Amherst). U.S. /12/615,717, (2009).

41 Allen, N. S.; Edge, M.; Wilkinson, A.; Liauw, C. M.; Mourelatou, D.; Barrio, J.; Martinez-Zaporta, M. A. Polym Degrad Stab 2000, 71, 113–122.

42 Luengo, C.; Allen, N. S.; Edge, M.; Wilkinson, A.; Parellada, M. D.; Barrio, J. A.; Santa, V. R. Polym Degrad Stab 2006, 91, 947–956.

43 Allen, N. S.; Edge, M.; Mourelatou, D.; Wilkinson, A.; Liauw, C. M.; Parellada, M. D.; Barrio, J. A.; Quiteria, V. R. S. Polym Degrad Stab 2003, 79, 297–307.

44 Ramaratnam, K.; Malphrus, J.; Luzinov, I. Polym Mater Sci Eng 2006, 95, 856–857.

45 Hilborn, J.; Ranby, B. Rubber Chem Technol 1988, 61, 568–576.

46 Hilborn, J.; Ranby, B. Rubber Chem Technol 1989, 62, 592–608.

47 Wang, W. Z. J Appl Polym Sci 2004, 93, 1837–1845.

48 Wang, W. Z.; Wu, Q. H.; Qu, B. J. Chem Res Chin Univ 2004, 20, 111–113.

49 ASTM. Standard test method for tensile properties of plastics by use of microtensile specimens, ASTM D 1708–02a, West Conshohocken, PA, 2002; p 3.

50 Munch, E.; Pelletier, J. M.; Sixou, B.; Vigier, G. Polymer 2006, 47, 3477–3485.

51 Whitby, G. S. Monographs on Industrial Chemistry—Plantation Rubber and the Testing of Rubber; Longmans Green and Co.: Manchester, London, 1920; p 459.